fermentation

MDPI

Article

Ferrous-Iron-Activated Sulfite-Accelerated Short-Chain Fatty Acid Production from Waste-Activated Sludge Fermentation: Process Assessment and Underlying Mechanism

Fang Cao [1], Xujiang Guo [1], Xiaoyun Yin [1], Zhixuan Cui [1], Shuli Liu [1] and Aijuan Zhou [1,2,*]

[1] College of Environmental Science and Engineering, Taiyuan University of Technology, Taiyuan 030024, China
[2] Shanxi Engineer Research Institute of Sludge Disposition and Resources, Taiyuan University of Technology, Taiyuan 030024, China
* Correspondence: zhouaijuan@tyut.edu.cn; Tel./Fax: +86-0351-3176581

Abstract: To break the bottlenecks of slow hydrolysis and low acid production efficiency of waste-activated sludge (WAS) in the traditional anaerobic fermentation process, this study investigated the employment of ferrous-iron (Fe(II))-activated sulfite to produce hydroxyl, sulfate, and other highly oxidizing radicals on WAS floc cracking and short-chain fatty acid (SCFAs) production during anaerobic fermentation. The effect of the dosage ratio of Fe(II)/S(IV) was also studied. Results showed that the combined pretreatment of Fe(II)-activated sulfite significantly promoted the exfoliation of extracellular polymers and the subsequent SCFAs production. The highest concentration of SCFAs reached 7326.5 mg COD/L under the optimal dosage of 1:2 for Fe(II)/S(IV), which was 1.1~2.1 times higher than that of other research groups. Meanwhile, the analysis by 3D fluorescence spectroscopy and EPR (electron paramagnetic resonance) showed that Fe(II)-activated sulfite had a synergistic effect on the rupture of sludge cells and the stripping of extracellular polymers, with SO_4^- and OH as the key radicals generated and being much stronger in the 1:1 and 1:2 groups. High-throughput sequencing showed that the Fe(II)-activated sulfite system significantly changed the functional microbial diversity. The anaerobic fermentation bacteria and sulfate-reducing bacteria were significantly enriched. The underlying mechanism of Fe(II)-activated sulfite oxidation and molecular ecological network of key microbiomes were unveiled.

Keywords: waste-activated sludge (WAS); short-chain fatty acids; ferrous-iron-activated sulfite; sulfate radicals; anaerobic fermentation

Citation: Cao, F.; Guo, X.; Yin, X.; Cui, Z.; Liu, S.; Zhou, A. Ferrous-Iron-Activated Sulfite-Accelerated Short-Chain Fatty Acid Production from Waste-Activated Sludge Fermentation: Process Assessment and Underlying Mechanism. *Fermentation* **2023**, *9*, 20. https://doi.org/10.3390/fermentation9010020

Academic Editor: Mohammad Taherzadeh

Received: 30 November 2022
Revised: 21 December 2022
Accepted: 23 December 2022
Published: 26 December 2022

1. Introduction

Greenhouse gas emissions led to global warming, and the world strives to limit carbon emissions and achieve carbon neutrality throughout the economic development process. With the promotion of the carbon neutrality goal, the future sludge treatment and disposal should be aimed at energy saving and energy resource recovery [1]. With the rapid development of China's national economy and the continuous improvement of urban productivity, the production of residual sludge, as the vital by-product of the biological treatment section of urban wastewater, has also increased in tandem with China's wastewater treatment capacity [2]. As a carrier of energy and resources, sludge contains a large amount of organic matter (such as proteins, carbohydrates, etc.) which can be utilized to realize sludge resources nationwide and reduce sludge disposal costs. Sludge contains a large number of pathogens, heavy metals, and other toxic and harmful substances, and its physical and chemical properties are unstable, so using traditional sludge treatment and disposal methods (sanitary landfill, incineration, land use, etc.) can cause secondary environmental pollution; for example, serious pollution of groundwater occurs from landfill leachate, and incineration produces dioxin [3]. In contrast, anaerobic fermentation with residual sludge as feedstock could not only realize harmless sludge treatment and quantity

reduction but also achieve resource recovery of residual sludge (e.g., short-chain fatty acids) [4,5]. SCFAs are high-value-added chemical substances that can be used to synthesize bioplastics [6]. In addition, SCFAs can be used as a carbon source for biological nitrogen and phosphorus removal in wastewater treatment plants [7], in microbial electrolytic cell (MEC) for hydrogen production [8], etc. However, the organic matter in sludge is encapsulated by cell walls and extracellular polymers (EPS), which makes its release difficult, and the hydrolysis stage becomes the rate-limiting step in anaerobic fermentation. For this reason, pretreatment methods such as thermal treatment [9,10], ultrasonication [11], enzymatic reaction [12], and chemical methods [13,14] have been proposed to accelerate the rate of sludge hydrolysis.

Advanced oxidation techniques (AOPs) are widely used for the oxidative degradation of substrates by generating highly reactive radicals, usually hydroxyl radicals (OH), which have a high redox potential. Advanced oxidation techniques based on sulfate radicals (SO_4^-) have received much attention for the degradation of pollutants and sludge pretreatment lysis cells due to their fast reaction rate and wide range of applications [15,16]. The oxidation capacity of SO_4^- (redox potential 2.5–3.1 V) was higher than that of OH (1.8–2.7 V), and the lifetime of SO_4^- was also higher than that of OH (half-life $t_{1/2}$ = 30~40 µs and $t_{1/2}$ < 1 µs, respectively) [17]. It exhibits a higher oxidation capacity than OH under neutral or alkaline conditions and a stronger radical for organic degradation [18]. SO_4^- is mainly generated by activating peroxynitrite (PMS) and persulfate (PDS), but PMS and PDS are expensive, which hinders their large-scale application, so SO_4^- can be generated by activating cheap and low-toxicity sulfite instead of PDS and PMS [19]. PDS can be activated by heat [20], UV [21], ultrasound [3], transition metals (Mn^{2+}, Co^{2+}, Cu^{2+}, etc.) [22] to produce SO_4^-. Excessive amounts of divalent iron may reduce the efficiency of radicals reactions by consuming large amounts of SO_4^-, while iron-based activators are widely used for sulfite activation because they are non-toxic, economical, and environmentally advantageous. Ai et al. found that the advanced oxidation system using Fe(II)/S(IV) could improve sludge dewatering performance [23], and Zhang et al. used Fe(II)/S(IV) to enhance the decolorization of Orange II [24]. However, the excess of divalent iron causes side reactions with SO_4^-, thus consuming SO_4^-, and the activation technique to optimize the Fe(II)/S(IV) ratio for acid production from anaerobic sludge fermentation has not been reported.

In this study, the Fe(II)-activated sulfite system was employed to regenerate SO_4^- and other free radicals to promote WAS solubilization. The influence of Fe(II)/S(IV) dosages on acidogenic fermentation of WAS were investigated by the whole process assessment, i.e., the release of extracellular polymers, the consumption of organics, the time-course of SCFAs production, and the influence of product spectrum. The underlying mechanisms were clarified by the diversity of functional microbes by Illumina Miseq sequencing, and the molecular ecological network of key microbiomes and the radical species were identified by electron paramagnetic resonance (EPR). This study provides a theoretical basis for the application of advanced oxidation technology on the resource recovery of waste biomass.

2. Materials and Methods

2.1. Experimental Materials

The experimental sludge was obtained from the sludge-thickening tank of Zhengyang Wastewater Treatment Plant in Jinzhong City, Shanxi Province, China, the sludge was filtered through a 200-mesh sieve, and the supernatant was removed after standing for 24 h and then placed in a refrigerator at 4 °C for backup. The remaining sludge was centrifuged at 10,000 rpm (11,180× *g*), and then the supernatant was filtered through a 0.45 µm membrane, followed by analysis and measurement of relevant indicators. The initial properties of the remaining sludge were: total suspended solid (TSS) 20.8 ± 0.3 g/L, volatile suspended solid (VSS) 11.1 ± 0.1 g/L, total chemical oxygen demand (TCOD) 20.7 ± 0.3 g/L, soluble chemical oxygen demand (SCOD) 0.19 ± 0.05 g/L, soluble proteins 42.3 ± 4.4 mg COD/L, soluble carbohydrates 18.5 ± 3.8 mg COD/L, NH_4^+-N 31.1 ± 1.6 mg/L, and pH 7.03 ± 0.1.

2.2. Experimental Set-Up

To investigate the effects of Fe(II)-activated sulfite system and the optimal Fe(II)/S(IV) dosages on the production of SCFAs from WAS anaerobic fermentation, six experimental groups were set-up as follows: Control (raw WAS, group 1), sole Fe(II) (group 2) and sulfite (group 3) were set as the control tests. Groups 5, 6, and 7 were Fe(II)/S(IV) = 1:1, 1:2, and 1:4 (g TSS/g TSS), respectively, and the dosage of sulfite was maintained at 800 mg S/L [25]. In this experiment, anaerobic serum bottles with a working volume of 400 mL were used. The fresh sludge from concentrated tank was added as inoculum to the serum bottles with a ratio of 1:10 (v/v), and the pH was adjusted and maintained with 7.0 $\pm$ 0.1 using 1.0 M NaOH or HCl, and nitrogen gas was introduced for 15 min to ensure an anaerobic environment. Each group was carried out in triplicates, and the reactors were placed in a constant temperature incubator at 35 °C and 120 rpm for around 20 days. Quantitative amounts of fermented WAS were centrifuged from the fermenters at 10,000 rpm (11,180$\times$ g) for 10 min every day. The supernatant was filtered through a 0.45 μm cellulose acetate membrane, and the contents of soluble organics, NH_4^+-N, and SCFAs were determined.

2.3. DNA Extraction and Illumina Miseq Sequencing

Total DNA was extracted from sludge samples using E.Z.N.A.™ Mag-Bind Soil DNA Kit (Sangon Biotech 138 bioengineering Co., Ltd., Shanghai, China). PCR amplification was performed by the DNA Services Facility with 341F-805R for V3–V4 regions of the bacterial 16S 140 rRNA genes, and the amplified DNA for each sample was sequenced by Illumina MiSeq platform. Key microbiomes of MENs based on random matrix theory were constructed and visualized by Cytoscape 3.7.2 software [26,27].

2.4. Analytical Methods

TSS, VSS, COD, phosphate, and NH_4^+-N were determined by standard methods (APHA 1998). The pH was determined by the glass electrode method. Soluble proteins were determined by the modified bicinchoninic acid (BCA) method [28], and the standard was bovine serum protein. Dissolved carbohydrates were determined by the phenol/sulfuric acid method, and the standard was glucose. Two layers of extracellular polymers, i.e., tightly-bound (TB-EPS) and loosely-bound EPS (LB-EPS), were extracted by thermal extraction [29], and the supernatant was filtered through a 0.45 μm membrane and then analyzed by 3D-EEM for semi-quantitative analysis. The radical species were identified by EPR with the spectrometer model JES-FA300 (JEOL, Akishima, Japan). Using 0.1 M of 5,5-dimethyl-1-pyrroline-N-oxide (DMPO) as a spin trapping agent, each system was trapped at 30 min of treatment [30]. SCFAs were determined by Agilent 6890 gas chromatograph with flame ionization detector. For comparative analysis, the above-measured concentrations (mg/L) were converted to COD concentration (mg COD/L) with the following conversion factors: 1.06 g COD/g (carbohydrate), 1.50 g COD/g (protein), 1.07 g COD/g (acetic acid, HAc), 1.51 g COD/g (propionic acid, HPr), 1.82 g COD/g (butyric acid, HBu), and 2.04 g COD/g (valeric acid, HVa). Significant influences at 0.05% level for the influence of Fe(II)/S(IV) dosages on acidogenic fermentation of WAS obtained through a one-way analysis of variance (ANOVA). Statistical analysis was performed by SPSS 19.0.

3. Results and Discussion

3.1. Exfoliation and Release of Extracellular Polymers in WAS Flocs

The release of proteins and carbohydrates in EPS can indirectly reflect the treatment efficiency of different pretreatments. The changes in soluble carbohydrates and proteins in the two EPS layers and dissolved organic matter (DOM) under different pretreatment groups are shown in Figure 1A. The soluble carbohydrate and protein contents in the Fe(II) group were significantly higher than those in the Control, but the Na_2SO_3 group did not release the organic matter content as much as the Fe(II) treatment. In the three

Fe(II)/S(IV)groups, the soluble carbohydrates and proteins in DOM increased with the increase in Fe(II)/S(IV) ratios and followed first-order kinetics Equations (1) and (2).

$$S_{pr} = 180.6\ ratio_{Fe/S} + 263.3\ R^2 = 0.9551 \quad (1)$$

$$S_{car} = 52.4\ ratio_{Fe/S} + 11.6\ R^2 = 0.9234 \quad (2)$$

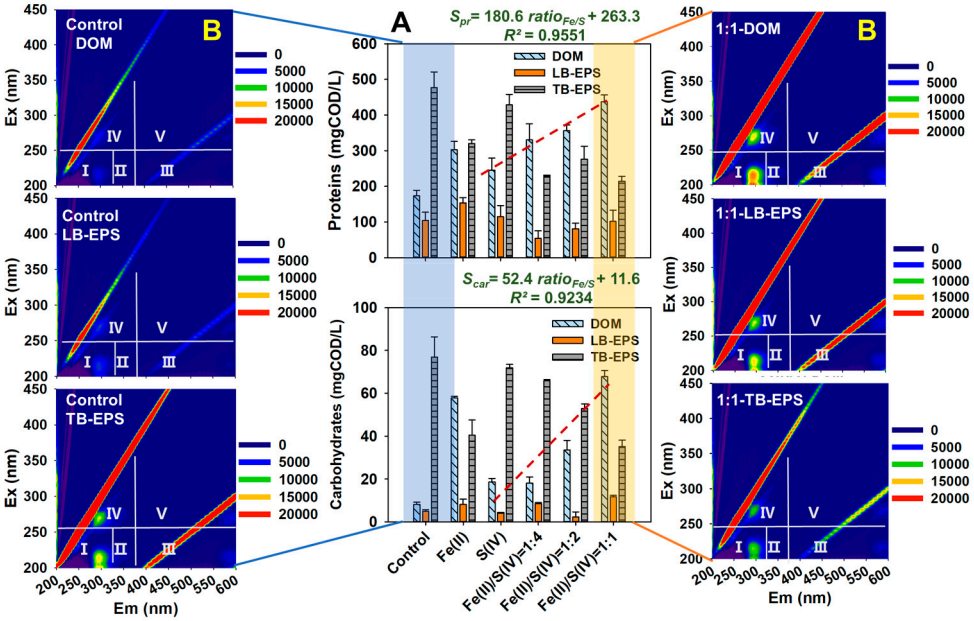

Figure 1. Changes in proteins and carbohydrates in the DOM, LB-EPS, and TB-EPS layers under different treatments of Fe^{2+}/Na_2SO_3 (**A**). 3D-EEM spectra of different layers in the RWAS and 1:1 Fe(II)/S(IV) tests (**B**).

Statistical significance calculations were used to contrast the different Fe(II)/S(IV) dosages in the Fe(II)-activated sulfite system. The coefficients of ANOVA were less than 0.05, which revealed that the Fe(II)/S(IV) dosages had a significant effect on release of proteins and carbohydrates in EPS. The maximum concentrations for the soluble carbohydrates and proteins, i.e., 68 and 437 mg COD/L, respectively, existed in the Fe(II)/S(IV) = 1:1 test, which were 1.0–8.4 and 1.2–2.5 folds higher than those in other experimental groups. Meanwhile, the amount of attached organic matter in TB-EPS was significantly reduced by the coupled Fe(II)/S(IV) oxidation. It indicates that the employed pretreatment can generate strong oxidizing radicals such as SO_4^- and OH to effectively promote the dissolution of sludge flocs, which in turn promotes the stripping of TB-EPS to release the organic matter into the liquid. Ai et al. investigated the synergistic effects of Fe(II)-activated sulfite oxidation and PAM flocculation on sludge dewaterability [23]. The organic matter content in LB-EPS was also increased, probably because LB-EPS, as an intermediate transport layer, had a loose and mobile structure. Some of the organics released from TB-EPS and cells was adsorbed in this layer.

The fluorescence intensities of DOM and EPS in raw and pretreated WAS by 1:1 Fe(II)/S (IV) were analyzed based on 3D-EEM spectra. The spectra were divided into five regions (I–V), which represented tyrosine-like protein, tryptophan-like protein, fulvic acid, dissolved microbial metabolites, and humic acid, respectively. Specifically, regions I and IV represented biodegradable organics, and regions II, III, and V represented non-biodegradable organic matter [30]. As shown in Figure 1B, the intensity of regions I and IV changed from weak to strong in the DOM test with Fe(II)/S(IV) = 1:1, which further indicated that the introduced pretreatment effectively enhanced the sludge cell rupture. A large amount of biodegradable organic matter was released into the liquid phase, enhancing

the biodegradability of the sludge. The fluorescence intensity was also enhanced in the intermediate transport layer LB-EPS. The decrease in fluorescence intensity in TB-EPS was attributed to the destruction of EPS structure, which led to the release of attached macromolecular organic matter into the DOM [31].

3.2. Changes in Soluble Organics during Fermentation

The concentration changes of soluble carbohydrates and proteins could reflect the solubilization of particulate organics embedded in the flocs. The coefficients of ANOVA were calculated by statistical significance of soluble carbohydrates and proteins (p = 0.201, p = 0.319). As shown in Figure 2A, the released soluble carbohydrates in DOM under five pretreatments showed sharply consumed from 2 d onward, which achieved the maximum consumption in the 1:1 Fe(II)/S(IV) test (57.8 mg COD/L). This was 1.2–12.5 folds higher than that under other pretreatments. With the prolongation of fermentation time, the soluble carbohydrates were further increased and then gradually decreased. More interestingly, this value in the 1:2 Fe(II)/S(IV) test peaked at 6 d (35.3 mg COD/L), which was followed by Fe(II) and 1:1 Fe(II)/S(IV) tests, whereas the soluble carbohydrates were slowly changed, indicating a balance of consumption and release existed during the whole fermentation of raw non-pretreated WAS.

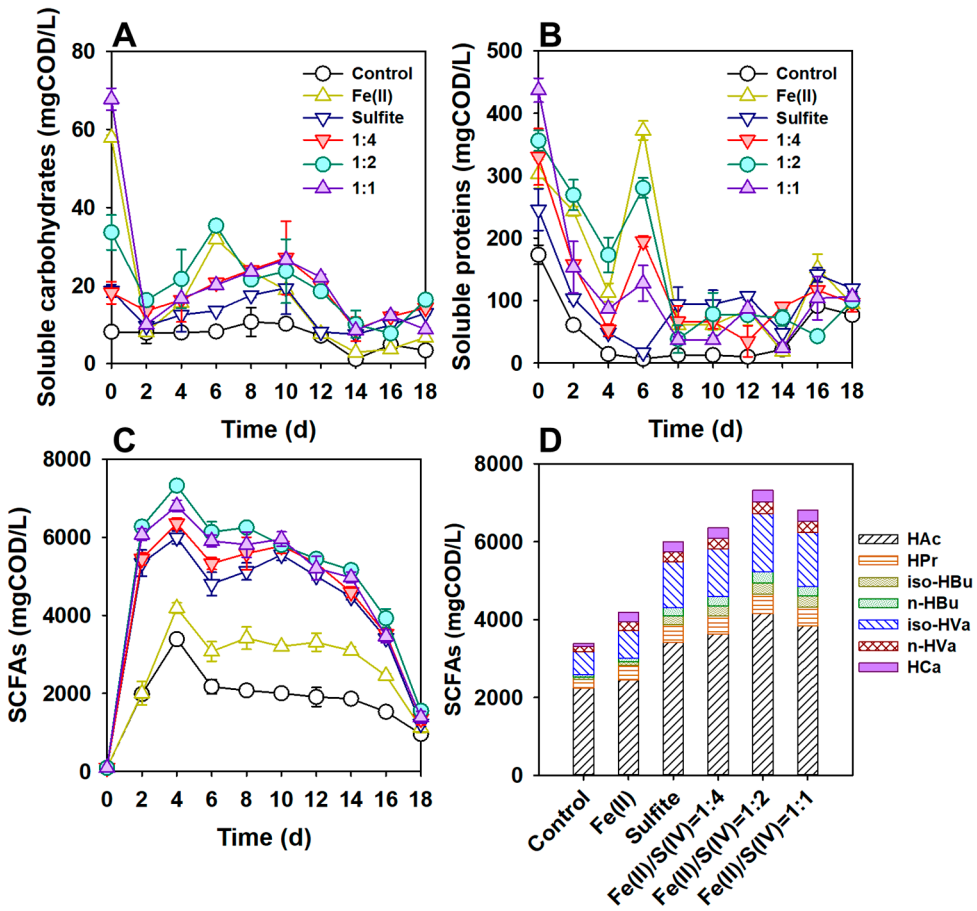

Figure 2. Time-courses of soluble organics during WAS fermentation under different pretreatments: soluble carbohydrates (**A**) and proteins (**B**). Time-courses of SCFAs concentrations (**C**) and the product spectrum on day 4 (**D**).

The trends of soluble proteins were basically consistent with that of carbohydrates (Figure 2B). In comparison, the first consumption phase continued to the fourth day. This may be related to the high activity of hydrolytic bacteria in the early stage of fermentation [32]. Concretely, the released soluble proteins achieved the highest level on day

6 and decreased with the on-going SCFAs recovery. Clearly, the combined Fe(II)/S(IV) pretreatment disrupts the cellular structure of the microorganisms, promoting the release of the aggregated and intracellular organic matter. Then, the dissolved organic matter produced at the initial fermentation stage is consumed by acid-producing bacteria, inducing a decreasing trend from day 6 onwards. This provides sufficient substrates for the growth of acid-producing bacteria during the subsequent fermentation and then promotes the production of SCFAs.

3.3. Influence of Fe(II)/S(IV) Dosages on Acidogenic Fermentation

The effects of different Fe(II)/S(IV) ratios on SCFAs production from WAS fermentation are shown in Figure 2C,D. The introduction of Fe(II)/S(IV) oxidation significantly enhanced the acidification efficiency. SCFAs concentration increased firstly and then decreased rapidly with fermentation time. The reason was the SCFAs production from the metabolism of small molecules, e.g., amino acids, polysaccharides, monosaccharides, etc. by fermentative acid-producing bacteria were further consumed by methanogens. This phenomenon commonly happens in mesophilic WAS fermentation [33]. Statistical significance calculations were used to contrast the influence of Fe(II)/S(IV) dosages on SCFAs production. The coefficients of ANOVA were less than 0.05, which revealed that the Fe(II)/S(IV) dosages had a significant effect on SCFAs production. The concentrations peaked on day 4 and maximized in the 1:2 Fe(II)/S(IV) test (7326.5 mg COD/L), which were 6808.5 and 6354.6 mg COD/L in the 1:1 and 1:4 tests, respectively. Liu et al. investigated the coupling sulfite (500 mg S/L) and alkaline (pH 9.5) pretreatments on SCFAs production from WAS and generated 324.8 $\pm$ 9.5 mg COD/g VSS (calculated to 7665.2 mg COD/L) [34]. That is, the performance of this work was comparable to the previous study. SCFAs concentrations in the sole Fe(II) group were not significantly different from that in the untreated WAS (Control), while the maximum concentration of SCFAs in the sole sulfite group achieved 5996.8 mg COD/L, which was 70% higher than that in the Control. The lower SCFAs concentration gained in the 1:1 Fe(II)/S(IV) test may be due to the inhibition effects of generated free radicals on the activity of acid-producing bacteria.

The distribution of maximum SCFAs generated in each experimental group on day 4 was shown in Figure 2D. HAc and HPr, as the main products of anaerobic fermentation, accounted for 64–73% in each group, which can serve as a promising and ideal carbon source for the denitrifying and phosphate-accumulating organisms during the wastewater treatment process. The coefficients of ANOVA were less than 0.05, which revealed that the Fe(II)/S(IV) dosages had a significant effect on HAc and HPr production. What was noteworthy was that 4154 and 502 mg COD/L HAc and HPr were generated in the 1:2 Fe(II)/S(IV) test, respectively, in contrast with 3418 and 449 mg COD/L in the sole sulfite test. It seems that the introduction of Fe(II) could efficiently promote HAc accumulation. Meanwhile, Fe(II)-activated sulfite pretreatment enhanced the HBu-type fermentation. In particular, the percentages of HBu content in the sole Fe(II) and untreated WAS groups accounted for 5.4% and 3.6%, respectively. The existence of sulfite and its derived chemicals seemingly caused the generation of HBu, with the proportions of all of the remaining four groups achieving around 7.6%. The reason behind this maybe that these free radicals and sulfur compounds hampered the bioconversion of HBu, or the generation rate of HBu was higher than the consumption rate. By comparison, the introduction of sulfite decreased the proportion of HVa from 27.7% to around 24.1% in the sole sulfite and Fe(II)/S(IV) tests.

3.4. Microbial Community Diversity and MENs Analysis

Illumina Miseq sequencing of microorganisms at the end of fermentation was performed to understand the diversity and similarity among the functional flora of the samples under different pretreatment systems. Figure 3A shows the shared OTUs of the six sludge samples. The shared OTUs of the six groups were 593, which accounted for 25.4% of the total OTUs (2337). Among them, the shared OTUs were mainly distributed in the phyla (in

order of abundance) Proteobacteria (35.27%), Chloroflexi (15.43%), Actinobacteria (13.01%), Bacteroidetes (12.94%), Firmicutes (9.79%), and Acidobacteriota (3.44%).

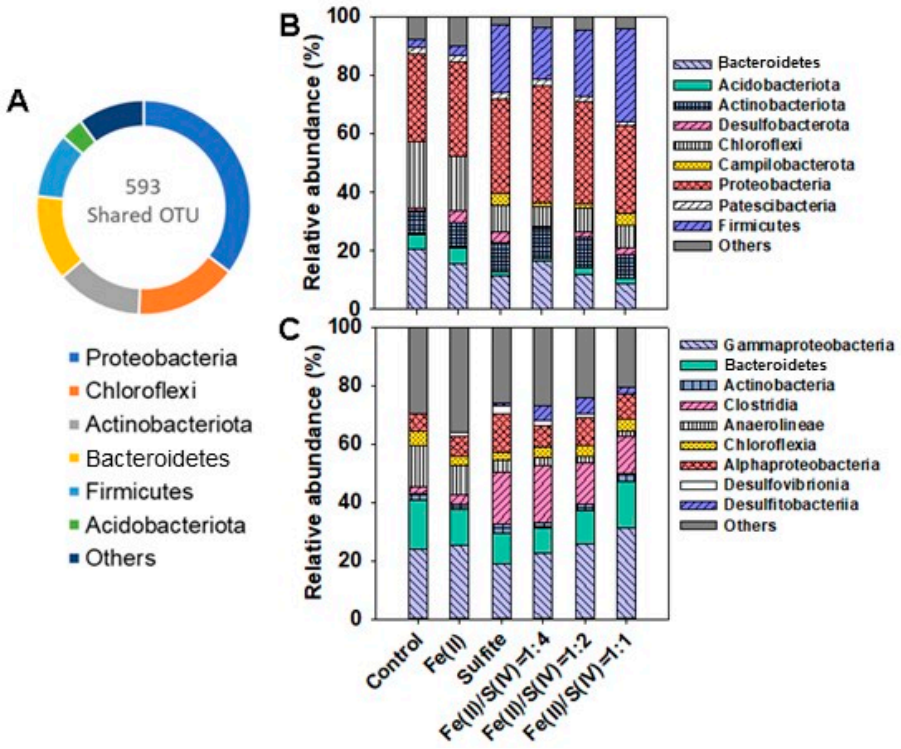

Figure 3. Shared OTU analysis of the six WAS samples (**A**). Relative abundance of functional bacteria at phylum (**B**) and class (**C**) levels.

The diversity and distribution among microbial communities were further investigated for phyla, class, and genera (Figures 3 and 4). Proteobacteria, Firmicutes, and Bacteroidetes were the common dominant phylum in anaerobic fermentation systems, with a cumulative abundance of 51.3–74.0% (Figure 3B). The percentage of Bacteroidetes decreased with the sole and coupling pretreatments (20.5% versus 8.7–16.5%), while Firmicutes and Proteobacteria increased. Among them, the Proteobacteria, as the dominant phylum of hydrolytic acidification, achieved the highest proportion in the coupling Fe(II)/S(IV) pretreated sample, increasing 0.34–9.97% compared with the untreated group. According to previous studies, Firmicutes were closely related to anaerobic hydrolysis and acidification processes [35], reaching the maximum in the Fe(II)/S(IV) 1:1 test (31.6% versus 2.6% in Control). This meant that sufficient organic substrates provided by the coupling oxidation led to strong hydrolytic activity in the pretreated WAS system [2].

Figure 3C shows the distribution of microbial communities in different fermentation groups at the class level. The dominant microbes were mainly distributed in the following five classes, i.e., Gammaproteobacteria, Alphaproteobacteria, Bacteroidia, Clostridia, and Anaerolineae. Gammaproteobacteria increased in proportion by 5.5–8.5% after the 1:1 Fe(II)/S(IV) pretreatment. Bacteroidia and Clostridia were the crucial species for the degradation of macromolecular organics to produce small molecule organic acids (e.g., HAc and HPr) [36], with the relative abundance from 2.09% (Control) to 12.8–19.4% in the coupling pretreatment groups. The percentage of Anaerolineae (Chloroflexi phylum) decreased significantly when Na_2SO_3 was dosed. Desulfitobacteriia was associated with the reduction of sulfate [37], and the relative abundance was minimal in the Control and Fe(II) groups but increased by 2.1–5.6% in the groups pretreated with Fe(II)/S(IV) oxidation.

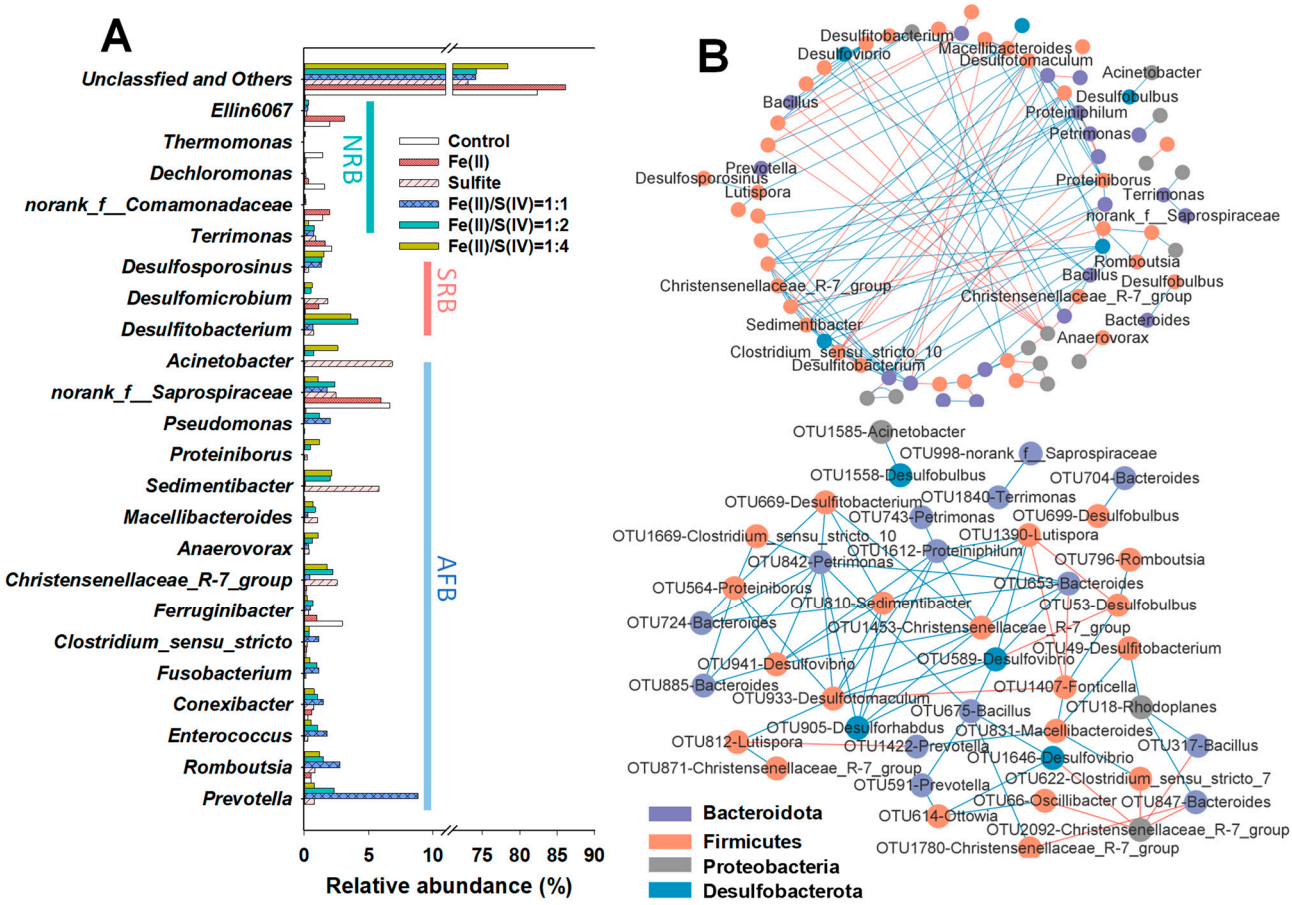

Figure 4. Relative abundance of functional bacteria at genus level (**A**). Molecular ecological network visualization of OTUs from functional microbial consortia (**B**).

As shown in Figure 4A, at the genus level, the total relative abundances of anaerobic hydrolyzing fermentative bacteria (AFB), e.g., *Prevotella*, *Romboutsia*, *Clostridium_sensu_stricto*, and *Pseudomonas*, were clearly magnified in the WAS fermentation systems pretreated by Fe(II)/S(IV) = 1:1, 1: 2, and 1:4 dosing ratios with a total proportion of 20.7%, 17.5%, and 15.1%, respectively. *Prevotella* was associated with the catabolism of dissolved carbohydrates and enriched with a relative abundance of 8.85% in 1:1 Fe(II)/S(IV) test, which was 3.8–10.9 times higher than that in Control, sole Fe(II) or S(IV), and other coupling pretreated tests. *Romboutsia*, *Enterococcus,* and *Clostridium_sensu_stricto,* which could both utilize a variety of organic substrates with HAc as the predominant product, predominated in the 1:1 Fe(II)/S(IV) test, with 2.8%, 1.8%, and 1.1%, respectively. It has been demonstrated that *Pseudomonas* can excrete depolymerase and extracellular protease to promote sludge hydrolysis [38]. *Desulfitobacterium*, *Desulfomicrobium*, and *Desulfosporosinus* were the functional microorganisms with sulfate-reducing ability [39] and were enriched in the Fe(II)/S(IV) groups. For example, the relative abundance of *Desulfosporosinus* achieved 1.4–1.6%, while it was not detected in the Control and sole Fe(II) tests. The proportion of *Desulfitobacterium* peaked in the 1:2 Fe(II)/S(IV) group (4.2%). In addition, the percentage of nitrate-reducing bacteria (NRB, e.g., *Terrimonas*, *Thermomonas*, *Dechloromonas*, etc.) in the Fe(II)/S(IV) tests all decreased. Some previous studies demonstrated the competitive relationship between NRB and SRB [40,41].

The MEN analysis of the Illumina Miseq results can further elucidate the intrinsic connections among the functional flora in anaerobic WAS fermentation systems. The overall topological properties and phylogeny of the microbial network are shown in Table 1 and Figure 4B.

Table 1. Major topological properties of the empirical networks.

Microbiome.	Similarity Threshold	Network Size	Links	Averaged Connectivity	Averaged Path Distance	Averaged Clustering Coefficient	Modularity (Fast Greedy)
Fermentation	0.97	76	134	3.526	3.839	0.102	0.551

The created network had 76 nodes (OTUs) that shared 134 links with each other. The network connectivity distribution fit well with the power-law model, with an R^2 of 0.846. The blue line indicates a positive correlation between nodes and the red line indicates a negative correlation between nodes. Extraction of sub-networks was used to further analyze the microbiological relationship (Figure 4B). There were significant positive correlations between AFB, i.e., *Prevotella* (OTU591 and OTU1422), *Bacillus* (OTU675), *Petrimonas* (OTU842 and OTU743), *Bacteroides* (OTU653, OTU885, and OTU724), *Proteiniphilum* (OTU1612), *Proteiniborus* (OUT564), *Christensenellaceae*_R-7_group (OTU1780), *Sedimentibacter* (OTU810), *Macellibacteroides* (OTU831), *Clostridium_sensu_stricto_7* (OTU622), and *Clostridium_sensu_stricto_10* (OTU1669), which reflected significant synergistic effects or similar ecological niche segregation existing among these functional microbes. *Desulforhabdus* (OTU905), *Desulfobulbus* (OTU1558), *Desulfitobacterium* (OTU669), *Desulfotomaculum* (OTU933), and *Desulfovibrio* (OTU589, OTU1646, and OTU941) were typical SRB, among which *Desulforhabdus* (OTU905) was associated with *Petrimonas* (OTU842), *Christensenellaceae_R-7_group* (OTU1453), and *Sedimentibacter* (OTU810). These suggested a possible symbiotic relationship between SRB and AFB. *Desulfovibrio* (OTU589), as an incomplete oxidative SRB that can oxidize ethanol to acetate and then reduce sulfate, was positively correlated with *Bacillus* (OTU675) and *Bacteroides* (OTU653), which were typical AFB and capable of producing lactate, acetate, and HBu from organics. Via the potential cooperative relationship between SRB and AFB, the inhibition on AFB by high hydrogen pressure could be alleviated when SRB was anticipated to consume extra hydrogen. Meanwhile, VFAs production, especially for HAc accumulation, was more likely to happen under thermodynamics principles.

3.5. Potential Mechanism of Fe(II)-Activated Sulfite Pretreatment for Accelerating WAS Acidogenic Fermentation

In the presence of Fe(II), $SO_{32}{}^{-}$ produced stable $FeHSO^{3+}$ and $FeSO_3{}^{+}$ complexes, and $FeSO_3{}^{+}$ acted as an initiator for the radical $SO_{32}{}^{-}$, whose decomposition was the rate-determining step of the whole chain reaction. $SO_3{}^{-}$ was then converted to $SO_5{}^{-}$ and subsequently generated a large amount of $SO_4{}^{-}$ and OH in the system through a series of chain reactions (Equations (1)–(8) and Figure 5A).

$SO_4{}^{-}$ and OH were the main contributors to EPS and cell wall disruption, destroying cell structure, promoting sludge disintegration, and releasing EPS and intra- and extracellular organic matter into the liquid phase to provide more substrate for subsequent fermentation of AFB [19,41]. It has been shown that the excess of Fe^{2+} reacts with $SO_4{}^{-}$ [19] Equation (9), so it was necessary to control the dosage ratio. As shown in Figure 5B, the EPR analysis of the pretreated sludge showed that DMPO-OH and DMPO-SO_4 signals were detected in all groups, and the intensities were stronger in the combined pretreatment group than that in the sole pretreatment groups, which was due to the activation of $SO_3{}^{2-}$ by the addition of Fe(II) enhanced the production of $SO_4{}^{-}$ and OH. This further provided an experimental basis for the above analysis.

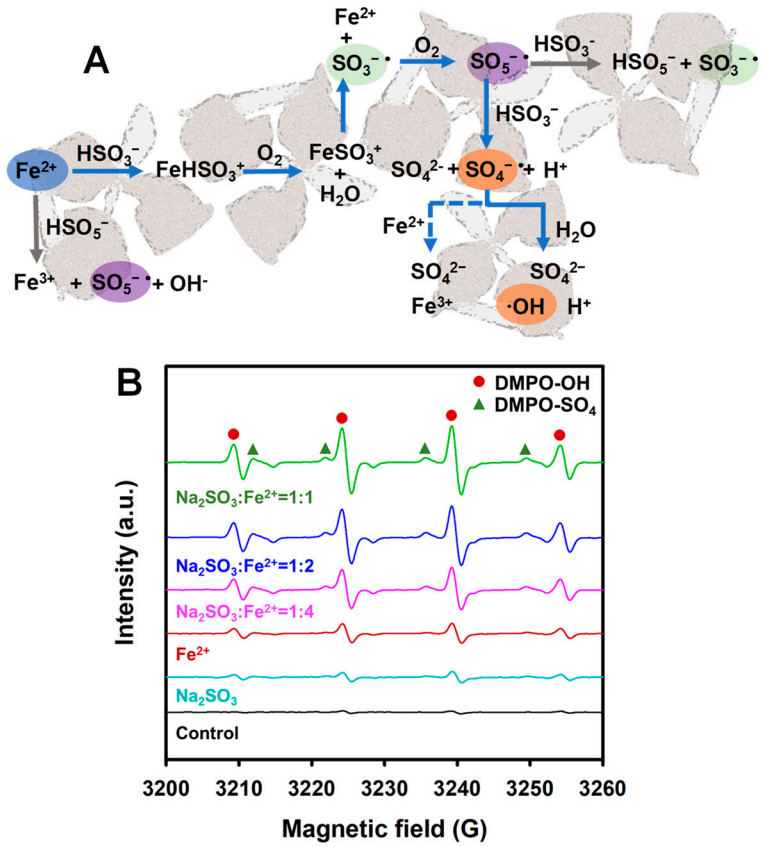

Figure 5. Schematic approach for the chain reactions (**A**) and EPR spectra (**B**) of Fe(II)/S(IV) oxidation system.

$$Fe^{2+} + HSO_3^- \rightarrow FeHSO_3^+ \; k_1 = 1 \times 10^4 \; M^{-1} \quad (3)$$

$$4FeHSO_3^+ + O_2 \rightarrow FeSO_3^+ + 2H_2O \; k_2 = 1.69 \times 10^3 \; M^{-1}s^{-1} \quad (4)$$

$$FeSO_3^+ \rightarrow Fe^{2+} + SO_3^- \cdot \; k_3 = 0.19 \; s^{-1} \quad (5)$$

$$SO_3^- \cdot + O_2 \rightarrow SO_5^- \cdot \; k_4 = 1.5 \times 10^9 \; M^{-1}s^{-1} \quad (6)$$

$$SO_5^- \cdot + HSO_3^- \rightarrow HSO_5^- + SO_3^- \cdot \; k_5 = 1.2 \times 10^4 \; M^{-1}s^{-1} \quad (7)$$

$$SO_5^- \cdot + HSO_3^- \rightarrow SO_4^{2-} + SO_4^- \cdot + H^+ \; k_6 \leq 4.8 \times 10^2 \; M^{-1}s^{-1} \quad (8)$$

$$Fe^{2+} + HSO_5^- \rightarrow Fe^{3+} + SO_5^- \cdot + OH^- \; k_7 = 3.0 \times 10^4 \; M^{-1}s^{-1} \quad (9)$$

$$SO_4^- \cdot + H_2O \rightarrow SO_4^{2-} + \cdot OH + H^+ \; k_{11} = \left(10^3 - 10^4\right) \; mol^{-1}Ls^{-1} \quad (10)$$

$$Fe^{2+} + SO_4^- \cdot \rightarrow SO_4^{2-} + Fe^{3+} \; k_8 = 9.9 \times 10^8 \; M^{-1}s^{-1} \quad (11)$$

4. Conclusions

This study firstly employed the coupling Fe(II)-activated sulfite oxidation on the SCFAs production from WAS fermentation. The optimal lysis and hydrolysis effects of sludge flocs and EPSs structure was appeared in the 1:1 Fe(II)/S(IV) test, and the maximum concentrations of soluble carbohydrates and proteins in DOM reached 67.8 and 437.1 mg COD/L, respectively. The Fe(II)/S(IV) oxidation effectively enhanced the production of SO_4^- and OH, which effectively promoted sludge cell rupture and disintegration of extracellular polymers, whereas the SCFAs concentrations peaked in the 1:2 Fe(II)/S(IV) test with HAc and HPr accounting for 66%. The underlying mechanism of the whole biotransformation

of WAS organics was explored by 3D-EEM and the molecular ecological networks among key microflora.

Author Contributions: F.C.: data curation, formal analysis, writing—original draft. X.G.: methodology, writing—review and editing. X.Y.: conceptualization. writing—review and editing. Z.C.: supervision. S.L.: visualization, project administration. A.Z.: resources, writing—review and editing. All authors have read and agreed to the published version of the manuscript.

Funding: This research was supported by the National Natural Science Foundation of China (NSFC, No. 52070139, 52270134, 52100155), the Shanxi-Zheda Institute of Advanced Materials and Chemical Engineering (No. 2022SX-TD006), the Central Government Guides the Special Fund Projects of Local Scientific and Technological Development (YDZJSX2022A008), the Natural Science Foundation of Youth Fund (No. 202103021222009), and the Scientific and Technological Project of Shanxi Province (No. 20210302124347).

Institutional Review Board Statement: Not applicable.

Informed Consent Statement: Not applicable.

Data Availability Statement: Not applicable.

Conflicts of Interest: The authors declare that they have no known competing financial interest or personal relationships that could have appeared to influence the work reported in this paper.

References

1. Zhang, C.; Yang, X.; Tan, X.; Wan, C.; Liu, X. Sewage sludge treatment technology under the requirement of carbon neutrality: Recent progress and perspectives. *Bioresour. Technol.* **2022**, *362*, 127853. [CrossRef] [PubMed]
2. Xu, Y.; Gong, H.; Dai, X. High-solid anaerobic digestion of sewage sludge: Achievements and perspectives. *Front. Environ. Sci. Eng.* **2021**, *15*, 71. [CrossRef]
3. Yang, Q.; Zhong, Y.; Zhong, H.; Li, X.; Du, W.; Li, X.; Chen, R.; Zeng, G. A novel pretreatment process of mature landfill leachate with ultrasonic activated persulfate: Optimization using integrated Taguchi method and response surface methodology. *Process Saf. Environ. Prot.* **2015**, *98*, 268–275. [CrossRef]
4. Wang, M.; Li, R.; Zhao, Q. Distribution and removal of antibiotic resistance genes during anaerobic sludge digestion with alkaline, thermal hydrolysis and ultrasonic pretreatments. *Front. Environ. Sci. Eng.* **2019**, *13*, 43. [CrossRef]
5. Appels, L.; Baeyens, J.; Degreve, J.; Dewil, R. Principles and potential of the anaerobic digestion of waste-activated sludge. *Prog. Energy Combust. Sci.* **2008**, *34*, 755–781. [CrossRef]
6. Pittmann, T.; Steinmetz, H. Potential for polyhydroxyalkanoate production on German or European municipal waste water treatment plants. *Bioresour. Technol.* **2016**, *214*, 9–15. [CrossRef]
7. Ji, Z.; Chen, Y. Using Sludge Fermentation Liquid To Improve Wastewater Short-Cut Nitrification-Denitrification and Denitrifying Phosphorus Removal via Nitrite. *Environ. Sci. Technol.* **2010**, *44*, 8957–8963. [CrossRef]
8. Liu, W.; Huang, S.; Zhou, A.; Zhou, G.; Ren, N.; Wang, A.; Zhuang, G. Hydrogen generation in microbial electrolysis cell feeding with fermentation liquid of waste activated sludge. *Int. J. Hydrogen Energy* **2012**, *37*, 13859–13864. [CrossRef]
9. Burger, G.; Parker, W. Investigation of the impacts of thermal pretreatment on waste activated sludge and development of a pretreatment model. *Water Res.* **2013**, *47*, 5245–5256. [CrossRef]
10. Castillo, A.; Ortega-Martinez, E.; Pages-Diaz, J.; Montalvo, S.; Huilinir, C. Micro-Aerobic Pre-Treatment vs. Thermal Pre-Treatment of Waste Activated Sludge for Its Subsequent Anaerobic Digestion in Semi-Continuous Digesters: A Comparative Study. *Fermentation* **2022**, *8*, 565. [CrossRef]
11. Li, X.; Guo, S.; Peng, Y.; He, Y.; Wang, S.; Li, L.; Zhao, M. Anaerobic digestion using ultrasound as pretreatment approach: Changes in waste activated sludge, anaerobic digestion performances and digestive microbial populations. *Biochem. Eng. J.* **2018**, *139*, 139–145. [CrossRef]
12. Song, Y.; Shi, Z.; Chen, S.Y.; Luo, L. Feasibility of using lysozyme to reduce excess sludge in activated sludge process. *J. Cent. South Univ.* **2013**, *20*, 2472–2477. [CrossRef]
13. Yu, Q.; Jin, X.; Zhang, Y. Sequential pretreatment for cell disintegration of municipal sludge in a neutral Bio-electro-Fenton system. *Water Res.* **2018**, *135*, 44–56. [CrossRef] [PubMed]
14. He, Z.-W.; Liu, W.-Z.; Gao, Q.; Tang, C.-C.; Wang, L.; Guo, Z.-C.; Zhou, A.-J.; Wang, A.-J. Potassium ferrate addition as an alternative pre-treatment to enhance shortchain fatty acids production from waste activated sludge. *Bioresour. Technol.* **2018**, *247*, 174–181. [CrossRef] [PubMed]
15. Fang, G.-D.; Dionysiou, D.D.; Wang, Y.; Al-Abed, S.R.; Zhou, D.-M. Sulfate radical-based degradation of polychlorinated biphenyls: Effects of chloride ion and reaction kinetics. *J. Hazard. Mater.* **2012**, *227*, 394–401. [CrossRef]

16. Yang, J.; Liu, X.; Wang, D.; Xu, Q.; Yang, Q.; Zeng, G.; Li, X.; Liu, Y.; Gong, J.; Ye, J.; et al. Mechanisms of peroxymonosulfate pretreatment enhancing production of short-chain fatty acids from waste activated sludge. *Water Res.* **2019**, *148*, 239–249. [CrossRef]
17. Li, J.; Li, Y.; Xiong, Z.; Yao, G.; Lai, B. The electrochemical advanced oxidation processes coupling of oxidants for organic pollutants degradation: A mini-review. *Chin. Chem. Lett.* **2019**, *30*, 2139–2146. [CrossRef]
18. Xia, X.; Zhu, F.; Li, J.; Yang, H.; Wei, L.; Li, Q.; Jiang, J.; Zhang, G.; Zhao, Q. A Review Study on Sulfate-Radical-Based Advanced Oxidation Processes for Domestic/Industrial Wastewater Treatment: Degradation, Efficiency, and Mechanism. *Front. Chem.* **2020**, *8*, 592056. [CrossRef]
19. Liu, C.; Chen, D.; Chen, X.e.; Wu, B. Application of zero-valent iron/sulfite system for aerobically digested sludge conditioning. *Chem. Eng. J.* **2021**, *420*, 127650. [CrossRef]
20. Kim, M.S.; Lee, K.-M.; Kim, H.-E.; Lee, H.-J.; Lee, C.; Lee, C. Disintegration of Waste Activated Sludge by Thermally-Activated Persulfates for Enhanced Dewaterability. *Environ. Sci. Technol.* **2016**, *50*, 7106–7115. [CrossRef]
21. Cao, Y.; Qiu, W.; Li, J.; Zhao, Y.; Jiang, J.; Pang, S. Sulfite enhanced transformation of iopamidol by UV photolysis in the presence of oxygen: Role of oxysulfur radicals. *Water Res.* **2021**, *189*, 116625. [CrossRef] [PubMed]
22. Zhou, D.; Chen, L.; Li, J.; Wu, F. Transition metal catalyzed sulfite auto-oxidation systems for oxidative decontamination in waters: A state-of-the-art minireview. *Chem. Eng. J.* **2018**, *346*, 726–738. [CrossRef]
23. Ai, J.; Wang, Z.; Dionysiou, D.D.; Liu, M.; Deng, Y.; Tang, M.; Liao, G.; Hu, A.; Zhang, W. Understanding synergistic mechanisms of ferrous iron activated sulfite oxidation and organic polymer flocculation for enhancing wastewater sludge dewaterability. *Water Res.* **2021**, *189*, 116652. [CrossRef] [PubMed]
24. Zhang, L.; Chen, L.; Xiao, M.; Zhang, L.; Wu, F.; Ge, L. Enhanced Decolorization of Orange II Solutions by the Fe(II)-Sulfite System under Xenon Lamp Irradiation. *Ind. Eng. Chem. Res.* **2013**, *52*, 10089–10094. [CrossRef]
25. Zan, F.; Zeng, Q.; Hao, T.; Ekama, G.A.; Hao, X.; Chen, G. Achieving methane production enhancement from waste activated sludge with sulfite pretreatment: Feasibility, kinetics and mechanism study. *Water Res.* **2019**, *158*, 438–448. [CrossRef]
26. Huang, C.; Liu, Q.; Li, Z.-L.; Ma, X.-d.; Hou, Y.-N.; Ren, N.-Q.; Wang, A.-J. Relationship between functional bacteria in a denitrification desulfurization system under autotrophic, heterotrophic, and mixotrophic conditions. *Water Res.* **2021**, *188*, 116526. [CrossRef]
27. Li, Z.-L.; Cheng, R.; Chen, F.; Lin, X.-Q.; Yao, X.-J.; Liang, B.; Huang, C.; Sun, K.; Wang, A.-J. Selective stress of antibiotics on microbial denitrification: Inhibitory effects, dynamics of microbial community structure and function. *J. Hazard. Mater.* **2021**, *405*, 124366. [CrossRef]
28. Zhou, A.; Wei, Y.; Fan, Y.; Shyryn, A.; Wang, S.; Liu, W.; Yuan, J.; Yue, X. Sulfate Reduction-Mediated Syntrophic Microbiomes Accelerated Waste-Activated Sludge Fermentation on the Basis of SO(4)(center dot-)Oxidation and Eliminated Superfluous Sulfate. *ACS Sustain. Chem. Eng.* **2020**, *8*, 9325–9334. [CrossRef]
29. Liu, Z.; Zhou, A.; Liu, H.; Wang, S.; Liu, W.; Wang, A.; Yue, X. Extracellular polymeric substance decomposition linked to hydrogen recovery from waste activated sludge: Role of peracetic acid and free nitrous acid co-pretreatment in a prefermentation-bioelectrolysis cascading system. *Water Res.* **2020**, *176*, 115724. [CrossRef]
30. Zhou, A.; Liu, H.; Varrone, C.; Shyryn, A.; Defemur, Z.; Wang, S.; Liu, W.; Yue, X. New insight into waste activated sludge acetogenesis triggered by coupling sulfite/ferrate oxidation with sulfate reduction-mediated syntrophic consortia. *Chem. Eng. J.* **2020**, *400*, 125885. [CrossRef]
31. Yin, Y.; Zhang, Y.; Karakashev, D.B.; Wang, J.; Angelidaki, I. Biological caproate production by Clostridium kluyveri from ethanol and acetate as carbon sources. *Bioresour. Technol.* **2017**, *241*, 638–644. [CrossRef] [PubMed]
32. Azman, S.; Khadem, A.F.; Van Lier, J.B.; Zeeman, G.; Plugge, C.M. Presence and Role of Anaerobic Hydrolytic Microbes in Conversion of Lignocellulosic Biomass for Biogas Production. *Crit. Rev. Environ. Sci. Technol.* **2015**, *45*, 2523–2564. [CrossRef]
33. Zhang, P.; Chen, Y.; Zhou, Q. Waste activated sludge hydrolysis and short-chain fatty acids accumulation under mesophilic and thermophilic conditions: Effect of pH. *Water Res.* **2009**, *43*, 3735–3742. [CrossRef] [PubMed]
34. Liu, X.; Du, M.; Yang, J.; Wu, Y.; Xu, Q.; Wang, D.; Yang, Q.; Yang, G.; Li, X. Sulfite serving as a pretreatment method for alkaline fermentation to enhance short-chain fatty acid production from waste activated sludge. *Chem. Eng. J.* **2020**, *385*, 123991. [CrossRef]
35. Fitamo, T.; Treu, L.; Boldrin, A.; Sartori, C.; Angelidaki, I.; Scheutz, C. Microbial population dynamics in urban organic waste anaerobic co-digestion with mixed sludge during a change in feedstock composition and different hydraulic retention times. *Water Res.* **2017**, *118*, 261–271. [CrossRef] [PubMed]
36. Wang, S.; Chen, L.; Yang, H.; Liu, Z. Influence of zinc oxide nanoparticles on anaerobic digestion of waste activated sludge and microbial communities. *RSC Adv.* **2021**, *11*, 5580–5589. [CrossRef]
37. Zhao, Q.; Li, X.; Wang, Y.; Cheng, Y.; Fan, W. Long-term bioremediation of cadmium contaminated sediment using sulfate reducing bacteria: Perspective on different depths of the sediment profile. *Chem. Eng. J.* **2023**, *451*, 138697. [CrossRef]
38. Muyzer, G.; Stams, A.J. The ecology and biotechnology of sulphate-reducing bacteria. *Nat. Rev. Microbiol.* **2008**, *6*, 441–454. [CrossRef]
39. Lai, R.; Li, Q.; Cheng, C.; Shen, H.; Liu, S.; Luo, Y.; Zhang, Z.; Sun, S. Bio-competitive exclusion of sulfate-reducing bacteria and its anticorrosion property. *J. Pet. Sci. Eng.* **2020**, *194*, 107480. [CrossRef]

40. Fan, F.; Zhang, B.; Liu, J.; Cai, Q.; Lin, W.; Chen, B. Towards sulfide removal and sulfate reducing bacteria inhibition: Function of biosurfactants produced by indigenous isolated nitrate reducing bacteria. *Chemosphere* **2020**, *238*, 124655. [CrossRef]
41. Xie, P.; Zhang, L.; Chen, J.; Ding, J.; Wan, Y.; Wang, S.; Wang, Z.; Zhou, A.; Ma, J. Enhanced degradation of organic contaminants by zero-valent iron/sulfite process under simulated sunlight irradiation. *Water Res.* **2019**, *149*, 169–178. [CrossRef] [PubMed]